THE JOURNAL OF BIOLOGICAL CHEMISTRY VOL. 281, NO. 33, pp. 23395–23404, August 18, 2006

Interdomain Communication in DNA Topoisomerase II

DNA BINDING AND ENZYME ACTIVATION[*S]

Received for publication, May 1, 2006, and in revised form, June 16, 2006 Published, JBC Papers in Press, June 16, 2006, DOI 10.1074/jbc.M604119200

Felix Mueller-Planitz and Daniel Herschlag[1]

From the Department of Biochemistry, School of Medicine, Stanford University, Stanford, California 94305-5307

Topoisomerase II catalyzes the ATP-dependent transport of a DNA segment (T-DNA) through a transient double strand break in another DNA segment (G-DNA). A fundamental mechanistic question is how the individual steps in this process are coordinated. We probed communication between the DNA binding sites and the individual enzymatic activities, ATP hydrolysis, and DNA cleavage. We employed short DNA duplexes to control occupancy at the two binding sites of wild-type enzyme and a variant with a G-DNA site mutation. The DNA concentration dependence of ATP hydrolysis and a fluorescence anisotropy assay provided thermodynamic information about DNA binding. The results suggest that G-DNA binds with higher affinity than T-DNA. Enzyme with only G-DNA bound is competent to cleave DNA, indicating that T-DNA is dispensable for DNA cleavage. The ATPase activity of enzyme bound solely to G-DNA is partially stimulated. Full stimulation requires binding of T-DNA. Both DNA binding sites therefore signal to the ATPase domains. The results support and extend current mechanistic models for topoisomerase II-catalyzed DNA transport and provide a framework for future mechanistic dissection.

DNA topoisomerase II is a molecular machine that resolves topological problems generated during DNA replication, transcription, recombination, chromosome segregation, and chromosome condensation (1). Topoisomerase II has attracted attention not only for its importance during cellular processes. It serves as a model system to mechanistically dissect allosteric, intramolecular communication of a complex molecular machine.

Biochemical and structural studies have suggested a mechanism for the overall catalytic mechanism of topoisomerase II (Fig. 1) (2, 3). According to this model, the enzyme binds to two different DNA segments. One segment, termed the gate or G-DNA, binds to the cleavage/religation domain (Fig. 1, step 1). The other DNA segment, termed the transported or T-DNA, binds and is trapped inside the enzyme when ATP binding induces a conformational change that clamps the ATPase domains around it (step 2). A transient double strand break is created in the G-DNA by two active site tyrosines that covalently attach to a 5′-phosphoryl group on each DNA strand. This break in the G-segment widens and acts as a gate through which the T-segment is transported (step 3), a step that is coupled to hydrolysis of ATP (4, 5). The cleaved G-DNA is religated, and the T-segment is released from the enzyme (step 4).

The catalytic functions of molecular machines, such as topoisomerase II, require the coordination of conformational changes. Such coordination can only be achieved if the regions of the enzyme that carry out the individual reaction steps can energetically communicate with one another. How these individual steps modulate one another and how they are integrated into the overall reaction mechanism is therefore central to understanding molecular machines.

Several aspects of the intramolecular communication in topoisomerase II have been established. For example, upon binding of ATP, the two ATPase domains of the enzyme self-associate (6–8) by exchanging an N-terminal "strap" motif that wraps around the ATP binding pocket of the neighboring subunit (9), demonstrating physical communication between the ATPase domains. DNA cleavage is stimulated in the presence of ATP, indicating that the ATPase and the DNA cleavage domains allosterically interact (4, 10, 11). However, the physical basis for the signaling between these domains is not known.

Although many aspects of the catalytic mechanism and interdomain communication of topoisomerase II have been established, fundamental questions about the intramolecular signaling mediating the coordinated DNA transport of topoisomerase II remain unresolved. It has been suggested, for example, that the enzyme must interact with the T-DNA before DNA bound at the G-DNA site can be cleaved (19). However, topoisomerase II with its ATPase gate "locked" was able to cleave linear DNA (6). This result is consistent with a requirement of T-DNA binding for DNA cleavage only if the DNA can thread into the enzyme to bind at both the T- and the G-DNA binding site (26).

Similar uncertainty exists regarding the influence of the DNA molecules on the other enzymatic activity, ATP hydrolysis. It is well established that the presence of DNA is sensed by the ATPase domains, since the ATPase activity increases in response to DNA binding (see, for example, Refs. 4, 12, and 13), but it has remained controversial whether binding the G-DNA at the DNA cleavage domains, the T-DNA between the ATPase domains, or both DNAs activate the ATPase reaction. Two lines of evidence suggest a role for the T-DNA in ATPase activation. First, mutation of a residue lining the putative T-DNA

* This work was supported by Boehringer Ingelheim Fonds (to F. M.-P.) and by National Institutes of Health Grant GM64798 (to D. H.). The costs of publication of this article were defrayed in part by the payment of page charges. This article must therefore be hereby marked "*advertisement*" in accordance with 18 U.S.C. Section 1734 solely to indicate this fact.

[S] The on-line version of this article (available at http://www.jbc.org) contains supplemental Schemes 1–4, Figs. S1–S7, and Table S1.

[1] To whom correspondence should be addressed: Stanford University, School of Medicine, Beckman Center B400, Dept. of Biochemistry, 279 Campus Dr., Stanford, CA 94305. Tel.: 650-723-9442; Fax: 650-723-6783; E-mail: herschla@cmgm.stanford.edu.

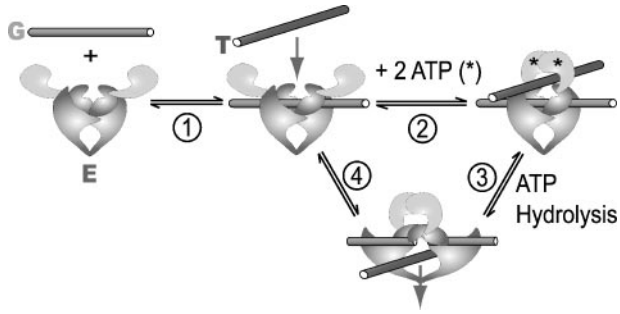

FIGURE 1. **Proposed mechanism of topoisomerase II catalyzed DNA transport (2, 3).** *G*, G-DNA; *T*, T-DNA; *E*, topoisomerase II (ATPase domains are *colored light gray*). Steps 1–4 are described in the Introduction.

site of the related enzyme *Escherichia coli* DNA gyrase abolished the stimulation of ATP hydrolysis by DNA (14). Second, DNA stimulated ATP hydrolysis by truncated topoisomerase II lacking the G-DNA binding site (8, 15–17). Olland and Wang (16) have proposed, however, that this stimulation occurs because DNA assists in dimerizing the truncated subunits in a manner that is not relevant to the normal reaction of the full-length enzyme and that the G-DNA is instead responsible for the DNA-dependent ATPase stimulation.

One of the basic challenges to dissecting communication within topoisomerase II is the presence of two DNA binding sites, which complicates interpretation of effects from DNA. To dissect the effects of G-DNA and T-DNA binding on the ATPase and DNA cleavage activity in intact, full-length topoisomerase II, the occupancy of the sites needs to be controlled. Plasmid DNA and long DNA duplexes can bind at one site or bend to allow binding of a single DNA at both sites. To ensure that a single DNA contacts only one binding site, we have used short DNA duplexes. Binding of these duplexes was probed by determining their effects on ATP hydrolysis and DNA cleavage and by measuring the fluorescence anisotropy change of dye-labeled duplexes. These experiments allow the DNA binding sites to be distinguished and provide information about allosteric communication between the DNA binding sites and the enzymatic activities of the enzyme. Most generally, the results allow evaluation and expansion of current mechanistic models of topoisomerase II-catalyzed DNA transport and provide a foundation for future mechanistic investigations.

EXPERIMENTAL PROCEDURES

Enzyme Expression and Purification—Full-length *Saccharomyces cerevisiae* topoisomerase II fused to an intein and a chitin binding domain affinity tag was expressed in the yeast strain BCY123. Chitin affinity chromatography and intein cleavage were performed essentially as described (18), followed by Heparin FF (Amersham Biosciences) and MonoQ (Amersham Biosciences) chromatography. See supplemental information for a detailed protocol.

Oligodeoxynucleotides and DNA Duplexes—Supplemental Table S1 summarizes the sequences of oligodeoxynucleotides (Integrated DNA Technologies) employed in this study. After annealing the corresponding top and bottom strands ($Oligo_{40}$top with $Oligo_{40}$bottom, $Oligo_{40}$top-ROX with $Oligo_{40}$bottom, $Oligo_{46}$ with itself, and $Oligo_{68}$top with $Oligo_{68}$bottom), the following duplexes were formed: a 40-bp duplex, a fluorescently labeled 40-bp duplex of the same sequence, a 46-bp duplex, and a 68-bp duplex. The duplexes are referred to throughout by their duplex length. The 68- and 40-bp-long DNA duplexes were derived from bp 63–130 and 87–126 in pBR322, respectively, and contain a known topoisomerase II cleavage site (19). The 46-bp duplex was selected because it was efficiently cleaved by the enzyme (see supplemental information).

Before annealing, all oligodeoxynucleotides were purified by denaturing PAGE except for the sequence $Oligo_{40}$top-ROX, which was purchased high pressure liquid chromatography-purified. As necessary, DNA duplexes were 5′-end-labeled with [γ-^{32}P]ATP (MP Biomedicals) and T4-polynucleotide kinase (New England Biolabs) according to the supplier's instructions. The 40-bp DNA duplex that carried the fluorescent dye 6-carboxy-X-rhodamine (ROX),[2] the 46-bp duplex, and ^{32}P-labeled duplexes were further purified by nondenaturing PAGE. The concentration of duplex DNA was determined by measuring the absorption of the individual nucleotides after exhaustive hydrolysis by *Crotalus atrox* phosphodiesterase I (Sigma) and DNase I (Roche Applied Science) (20).

The concentration of DNA duplex necessary to half-maximally stimulate the ATPase activity at enzyme concentrations low enough such that no or minimal sigmoidal shape of the DNA stimulation curve is observed ($[E] < 50$ nM; see Fig. 2 and supplemental Fig. S4) is referred to as K_M^{duplex} herein. The value of K_M^{duplex} was lower for the 68-bp duplex than the 46-bp and 40-bp duplex ($K_M^{68\ bp} = 0.15\ \mu M$, $K_M^{46\ bp} = 2.7\ \mu M$, and $K_M^{40\ bp} = 4\ \mu M$ with saturating ATP; Fig. 2, supplemental Fig. S4, and data not shown). The low K_M^{duplex} of the 68-bp duplex allowed the use of saturating concentrations of enzyme with respect to DNA in the ATPase assay.

Enzyme Assays—Reaction buffer (50 mM potassium Hepes, pH 7.5, 150 mM KOAc, 0.1 mM EDTA, 20% sucrose, 0.25 mg/ml BSA, 0.01% Tween 20, 5 mM 2-mercaptoethanol, and 10 mM $Mg(OAc)_2$ or $Ca(OAc)_2$) was employed throughout. This buffer prevented aggregation of topoisomerase II at concentrations less than 6 μM as judged by the absence of light scattering at wavelengths of >330 nm. Before each experiment, an aliquot of topoisomerase II was thawed and buffer-exchanged into reaction buffer minus BSA using an Amicon Ultra (Millipore) 100 kDa cut-off centrifugal filter at 4 °C. The enzyme was spun for 15 min in a microcentrifuge at 4 °C. The concentration of the enzyme in the supernatant was determined using the calculated molar extinction coefficient of 325,380 $M^{-1}\ cm^{-1}$ at 280 nm in 20 mM sodium phosphate (pH 6.5) and 6 M guanidinium hydrochloride (21). The active site titration using DNA duplexes shown in Fig. 4 suggested that a fraction (~25%; see below) of the enzyme does not cleave DNA. This result may reflect a fraction of the enzyme that is inactive or an inaccurate calculated extinction coefficient. The enzyme concentrations reported throughout are corrected for that fraction. All assays were performed at 30 °C.

[2] The abbreviations used are: ROX, 6-carboxy-X-rhodamine; BSA, bovine serum albumin; AMPPNP, 5′-adenylyl-β,γ-imidodiphosphate.

Steady State ATPase Assays—Steady state ATPase activity was measured in reaction buffer containing 10 mM Mg^{2+} with a coupled ATPase assay essentially as described (22) (see supplemental information for details). Steady state ATPase kinetic parameters (Table 1) were obtained as follows. K_M^{ATP} in the absence or presence of saturating 68-bp DNA (>0.8 μM for wild type and 5 μM for the Y782F variant) was measured by varying the ATP concentration and fitting the curves to the expression $k_{obs} = k_{max} \times [ATP]/(K_M^{ATP} + [ATP])$. Basal and DNA-stimulated k_{cat} values were obtained from the DNA stimulation curves in Figs. 2*A* and 3 (see description of the quantitative analysis below). The steady state ATPase kinetic parameters of wild-type enzyme measured in our reaction buffer are within 2–3-fold of published values (18). Side-by-side comparison showed that the differences relative to earlier measurements are primarily due to the addition of sucrose in our assays, which helped prevent enzyme aggregation (data not shown). Sucrose addition reduced the basal ATPase activity 2–3-fold while having little affect on the DNA-stimulated ATPase activity. The DNA-stimulated ATPase activity of the Y782F mutant is higher than reported, presumably because nonsaturating DNA concentrations have been employed previously (18).

DNA Cleavage Assay—Enzyme was mixed with trace amounts of the ^{32}P-labeled, 46-bp DNA duplex, varying amounts of unlabeled duplex, and, as indicated, saturating AMPPNP (0.5 mM). AMPPNP (Sigma) was purified before use (23). Reactions were quenched after 10 min by the addition of NaOH (0.5 M final concentration). Control experiments showed that doubling the incubation time or using an acid quench instead (0.2 M HCl) gave identical levels of cleavage. An SDS quench (1%) resulted in slightly lower levels of cleavage, suggesting that SDS is not a sufficiently rapid quench. The reaction mixtures quenched with NaOH were back-titrated to pH ~9 with 4 M Tris·HCl, pH 7, loading buffer was added (50 volumes of 9 M urea, 20% sucrose, 5 mM EDTA for reactions using 0.36 μM enzyme and 500 volumes for reactions using 3.2 μM enzyme), and the mixture was heated for 1 min at 90 °C. The radiolabeled cleavage products were separated from uncleaved oligonucleotides by denaturing gel electrophoresis (7 M urea, 14% acrylamide) and quantitated using PhosphorImager analysis (Molecular Dynamics) with ImageQuant quantitation software. Cleavage was completely reversible upon dilution of the sample or the addition of excess unlabeled DNA (data not shown). These and additional kinetic experiments[3] demonstrate the kinetic competence of the cleavage complexes.

Quantitative Analysis of ATPase and DNA Cleavage Data—Steady state ATPase and DNA cleavage data were fit to Schemes 1 and 2 using Matlab (The MathWorks). To this end, systems of linear equations were constructed based on the equilibria describing Schemes 1 and 2. The equations were solved for the concentration of each species as a function of the equilibrium constants and the total DNA and total enzyme concentrations. For each species, three possible solutions describing its equilibrium concentration were obtained. The relevant solution for a given set of parameters was selected by enforcing the following side conditions; the solution was not allowed to have imaginary parts, be negative, or be greater than the maximum possible concentration given by the total enzyme and DNA concentrations.

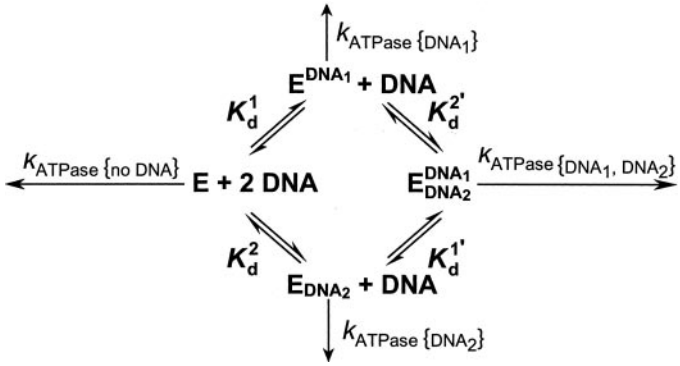

SCHEME 1 Steady state ATPase reaction

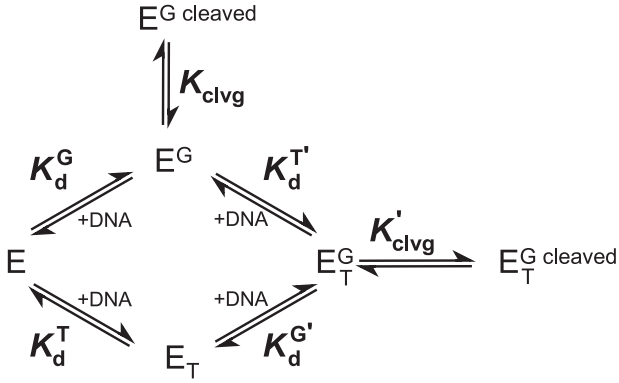

SCHEME 2 DNA cleavage reaction

The expected ATPase activity for a given set of dissociation constants and total DNA and enzyme concentrations was calculated in the following way. Each of the four species in Scheme 1 was assigned a k_{cat} and K_M^{ATP} value (see below). The ATPase activity of this species was calculated by multiplying its equilibrium concentration by the expression $k_{cat} \times [ATP]/(K_M^{ATP} + [ATP])$. The individual ATPase activities of all four species were summed and normalized by the total enzyme concentration. The K_m values for ATP of free enzyme and enzyme bound to two DNAs ($K_{M\ (no\ DNA)}^{ATP}$ and $K_{M\ (DNA_1,\ DNA_2)}^{ATP}$, respectively) were measured directly in independent experiments in the absence and presence of saturating DNA (Table 1). Similarly, the k_{cat} values for free enzyme and $E_{DNA_2}^{DNA_1}$ ($k_{cat\ (no\ DNA)}$ and $k_{cat\ (DNA_1,\ DNA_2)}$) are given by the ATPase activity in the absence of DNA and the activity obtained at saturating DNA. For E_{DNA_1} and E_{DNA_2}, k_{cat} and K_M^{ATP} values were assumed as indicated. The ATPase data obtained at various enzyme concentrations were globally fit in Matlab using a nonlinear least squares algorithm.

To fit the DNA cleavage data (Fig. 4, supplemental Fig. S6), the equilibrium concentrations of $E^{G\ cleaved}$ and $E_T^{G\ cleaved}$ were first calculated for a given set of total enzyme and DNA concentrations and equilibrium constants defined in Scheme 2.

[3] F. Mueller-Planitz and D. Herschlag, unpublished results.

TABLE 1
Steady state kinetic parameters for hydrolysis of ATP
Reactions were performed as described under "Experimental Procedures."

Topoisomerase II construct	DNA[a]	k_{cat}	K_M^{ATP}
		s^{-1}	mM
Wild type	−	0.23	1.0
Wild type	+	7.2	0.2
Y782F	−	0.28	1.0
Y782F	+	5.6	0.25

[a] 68-bp DNA duplex (see supplemental Table S1 for sequence).

The observed fraction of cleaved DNA was then related to the model of Scheme 2 according to the following equation.

$$\text{Fraction cleavage} = ([E^{G\,cleaved}] + [E_T^{G\,cleaved}])/[DNA]_{total} \quad \text{(Eq. 1)}$$

In addition to the equilibrium constants describing the scheme, the fraction of enzyme not capable of cleaving DNA was allowed to vary in the fits, since a fraction of the enzyme might be inactive, or the calculated extinction coefficient used to determine the enzyme concentration might be inaccurate. Best fits were achieved with a fraction of the enzyme incapable of cleaving DNA of ~0.25, and values above 0.5 did not fit the data well based on a χ^2 goodness of fit test and on visual inspection of fits (Fig. 4, *A* and *B*, and data not shown). An upper limit of 0.5 for the enzyme concentration not capable of cleaving DNA was used for the fits in Fig. 4*C*.

Fluorescence Anisotropy Measurements—Equilibrium fluorescence anisotropy measurements were acquired using a T-format FluoroLog-3 spectrofluorometer (HORIBA Jobin Yvon) in a 45-μl microcuvette (Starna Cells). The excitation wavelength (550 nm) and the S-emission channel wavelength (602 nm) were selected with monochromators using 10-nm band paths. In the T-emission channel, scattered light was suppressed with a 590-nm long pass filter. Subnanomolar concentrations (see below) of ROX-labeled 40-bp DNA were mixed with varying concentrations of enzyme and incubated for 3 min before each measurement. Longer incubation times did not alter the measured anisotropy values. The fluorescence intensity of the ROX-labeled DNA measured under magic angle conditions did not change upon binding of the DNA to enzyme. The data were fit to the quadratic binding isotherm in Equation 2 using nonlinear regression analysis in Matlab.

$$r_{obs} = (r_{bound} - r_{free})\frac{[E_T] + [DNA_T] + K_d - \sqrt{([E_T] + [DNA_T] + K_d)^2 - 4[E_T][DNA_T]}}{2[DNA_T]} + r_{free} \quad \text{(Eq. 2)}$$

In Equation 2, r_{obs}, r_{free}, and r_{bound} refer to the observed anisotropy, the anisotropy of the DNA free in solution, and the anisotropy of the DNA bound to enzyme, respectively. K_d is the affinity, and $[E_T]$ and $[DNA_T]$ are the total enzyme and DNA concentrations used. Binding isotherms were obtained for wild type and the Y782F mutant at 0.8 nM DNA (Fig. 5 and data not shown). This DNA concentration is subsaturating for the wild-type but not for the mutant enzyme. The equilibrium binding experiment was therefore repeated with a lower DNA concentration (0.16 nM) for the mutant enzyme (Fig. 5). The K_d values determined at the two DNA concentrations for the mutant (0.31 and 0.14 nM, respectively) are within about 2-fold of one another. Possible interactions between the ROX fluorophore and the enzyme were controlled for by comparing the affinities obtained from binding fluorophore-labeled DNA to the enzyme and from a competition experiment between fluorophore-labeled and varying concentrations of unlabeled DNA. The observed affinity from the competition experiment was corrected as described (24). K_d values obtained from the two methods were within 2-fold of one another, suggesting at most a modest interaction of the fluorophore with the enzyme (data not shown).

DNA binding was previously monitored using a filter binding assay with 2 nM ^{32}P-labeled 46-bp DNA and varying enzyme concentrations under low ionic strength conditions (18). However, the enzyme solubility is low under these low ionic strength conditions (<40 nM in 25 mM Hepes-KOH, pH 7.5, 5 mM $MgCl_2$, 50 mM KCl, 6% glycerol, 5 mM 2-mercaptoethanol; data not shown). Therefore, the reported K_d values (11 nM for wild type and Y782F mutant) probably represent upper limits. Our own binding measurements using the fluorescence anisotropy assay under these buffer conditions confirm that the dissociation constants for both enzymes are lower than previously reported (<2 nM for wild-type and the Y782F mutant enzyme with ROX-labeled 40-bp DNA; supplemental Fig. S7). These values are limits, since the binding curves may represent stoichiometric titrations of DNA with enzyme. The aggregation propensity of the enzyme and limited signal prevented more accurate data from being obtained or measuring binding with lower concentrations of DNA under these low ionic strength conditions.

RESULTS

The goal of the experiments described herein was to thermodynamically distinguish the two DNA binding sites, to obtain information on the communication of these sites with the ATPase and DNA cleavage activities, and to provide a foundation for future mechanistic dissection. An ability to selectively occupy the G-DNA or the T-DNA binding sites on topoisomerase II is essential to dissect the roles of the two DNAs in activating the enzymatic activities. To enrich only a single site, we have used short DNA duplexes and employed ATP turnover, DNA cleavage, and a fluorescence anisotropy-based DNA binding assay as readouts for DNA binding.

DNA-stimulated ATPase Activity: Thermodynamic Information about the Two DNA Binding Sites—The stimulation of ATP hydrolysis by DNA provides valuable thermodynamic information about DNA binding. For example, a sigmoidal curve for DNA stimulation of the ATPase activity was observed for *E. coli* DNA gyrase. This sigmoidal shape suggests that two DNA duplexes are bound in the activated complex (27). The DNA concentration dependence of ATP hydrolysis also contains information about the affinities for the DNA binding sites, as presented below.

We analyzed the effect of a 68-bp DNA duplex on the ATP hydrolysis rate (see supplemental Table S1 for DNA sequences). This duplex is long enough to bind with high affinity to the enzyme (see below) but not long enough to contact both DNA binding sites simultaneously (see below, and see Ref. 27). The high affinity allows the use of enzyme concentrations that are above the affinities for both DNA binding sites, and

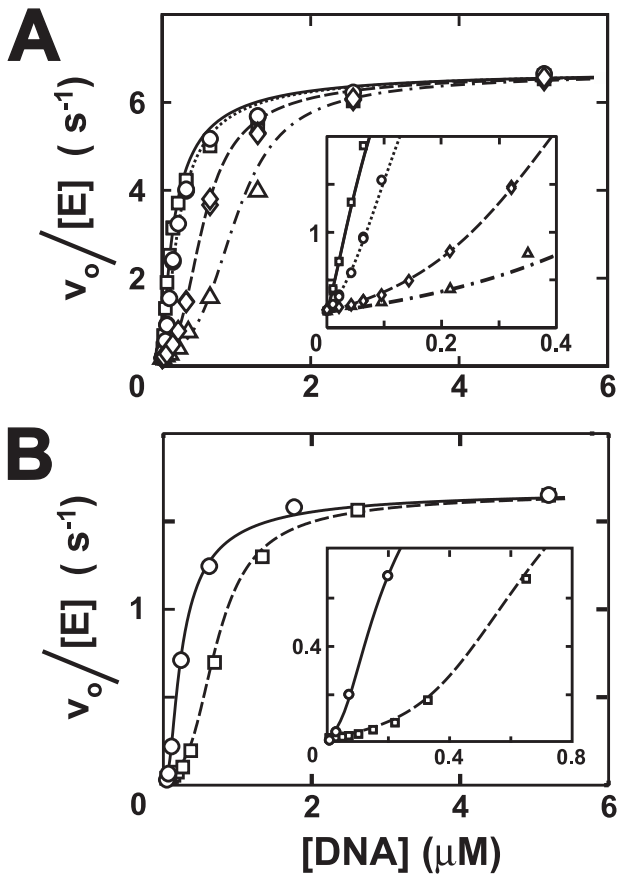

FIGURE 2. **Dependence of the observed ATP hydrolysis rate constant (v_o/[*E*]) on the concentration of the 68-bp DNA duplex at varying concentrations of topoisomerase II with saturating (*A*; 3 mM) or subsaturating (*B*; 60 μM) Mg^{2+}-ATP.** Enzyme concentrations were as follows: 13 nM (□), 65 nM (○), 325 nM (◇), and 650 nM (△) (*A*) and 65 nM (○) and 400 nM (□) (*B*). The *lines* represent a global fit of the data to Scheme 1.

these conditions provide the highest signal for the analysis below.

Rates of ATP hydrolysis as a function of DNA concentration were obtained at a series of enzyme concentrations with saturating and subsaturating concentrations of Mg^{2+}-ATP (Fig. 2). Plots of the ATP hydrolysis rate *versus* the DNA concentration are sigmoidal, and the DNA concentration at which the inflection of the curves occur increased with increasing enzyme concentration. The sigmoidal shape of the data indicates that more than one DNA is required to fully stimulate the Mg^{2+}-ATPase activity. The requirement for higher concentrations of DNA to observe stimulation with higher concentrations of enzyme present indicates that an enzyme-DNA complex accumulates that gives no or only fractional stimulation and that the weaker binding site is stimulatory. These conclusions are underscored by the quantitative models described below and in the supplemental information.

We interpret the DNA dependence of the ATPase activity with models that postulate the existence of two DNA binding sites, consistent with biochemical data, mechanistic considerations, and x-ray structures of topoisomerase II and related enzymes (Scheme 1) (6, 14, 28, 29). In the simplest model that accounts for the data of Fig. 2, binding of a single DNA to one binding site, described by K_d^1, leaves the ATPase activity unperturbed ($k_{\text{ATPase (no DNA)}} = k_{\text{ATPase (DNA}_1\text{)}}$, Scheme 1), whereas binding of DNA to the site described by K_d^2 activates ATP hydrolysis to the same level as with both DNA binding sites occupied ($k_{\text{ATPase (DNA}_2\text{)}} = k_{\text{ATPase (DNA}_1\text{, DNA}_2\text{)}}$). Because the DNA stimulation curves are sigmoidal (Fig. 2), the data require preferential occupancy of the nonstimulatory binding site (K_d^1) relative to the stimulatory site (K_d^2; $K_d^1 < K_d^2$). Quantitative analysis of the data confirms the consistency of this model with the data (Fig. 2, *lines*), whereas models in which the affinity of the stimulatory site exceeds that of the nonstimulatory site do not reproduce the sigmoidal shape of the stimulation curves (supplemental Fig. S2 and data not shown).

TABLE 2
DNA affinity estimates

Affinity estimates were derived from the analysis shown in supplemental Fig. S3. Equilibrium constants are defined in Scheme 1. The given range of values represents conservative limits that include all values that can fit the data with at least 5% probability according to a χ^2 goodness of fit test.

	Wild-type enzyme			Y782F enzyme; 68-bp duplex[a]; saturating [ATP][d]
	68-bp duplex[a]		40-bp duplex[a]; saturating [ATP][d]	
	Saturating [ATP][b]	Subsaturating [ATP][c]		
K_d^1 (nM)	6–70	<60	100–2000	<150
K_d^2 (nM)	$\geq K_d^1$	$\geq K_d^1$	$\geq K_d^1$	$\geq K_d^1$
$K_d^{1'}$ (nM)	$\leq K_d^{2'}$	$\geq K_d^1$	$\geq K_d^1$	$\geq K_d^1$
$K_d^{2'}$ (nM)	50–240	40–550	1100–6000	550–6000

[a] See supplemental Table S1 for sequence.
[b] 3 mM Mg^{2+}·ATP.
[c] 0.06 mM Mg^{2+}·ATP.

The simple model presented above posits that DNA binding to one of the two binding sites is necessary and sufficient for maximal stimulation of ATP turnover. However, we considered alternative models in which ATP hydrolysis is affected by DNA bound at either site ($k_{\text{ATPase (DNA}_1\text{)}} > k_{\text{ATPase (no DNA)}}$ and $k_{\text{ATPase (DNA}_1\text{, DNA}_2\text{)}} > k_{\text{ATPase (DNA}_2\text{)}}$). In all cases, ATPase stimulation from a complex with two bound DNAs is required to fit the data. Nevertheless, a range of possible contributions of each binding site to ATPase stimulation is possible. Binding of DNA to the higher affinity binding site alone could stimulate the ATPase activity up to 10-fold. No limit for the stimulation provided by binding of only the lower affinity DNA can be determined by the available data, since successively weaker binding of DNA to this site alone (K_d^2) can be postulated and would give successively higher upper limits for the ATPase activity of this species ($k_{\text{ATPase (DNA}_2\text{)}}$; supplemental Fig. S2). The analysis also provides estimates for the DNA affinities in Scheme 1 (supplemental Fig. S3; K_d^1 was defined to be of smaller or equal value as K_d^2 in this analysis so that it always refers to the high affinity DNA site). As summarized in Table 2, estimates or limits for dissociation constants are obtained in some cases, and in others the values are established relative to the other dissociation constants. Inspection of Table 2 shows that binding of a second DNA at site 2 ($K_d^{2'}$) (*i.e.* DNA binding after DNA occupies site 1) cannot be much stronger than binding of the first DNA. The situation in which $K_d^{2'} < K_d^1$ is referred to as *observed* cooperativity herein.

To test if basic conclusions derived from the analysis using the 68-bp DNA apply to shorter DNAs, we employed a 40-bp duplex. A sigmoidally shaped DNA stimulation curve was also observed for the shorter duplex (supplemental Fig. S4). Similar

to the 68-bp duplex data, the upturn of the curves occurred at higher DNA concentrations with higher enzyme concentrations, and quantitative analysis yielded dissociation constants and relationships analogous to those obtained with the 68-bp duplex (supplemental Fig. S3 and Table 2).

In summary, these results revealed that there is no strong, observed DNA binding cooperativity. Hence, it is possible to enrich topoisomerase bound to a single DNA duplex, a property that we exploit below to determine which binding sites need to be occupied to allow DNA cleavage and to identify the binding site with the higher affinity. Moreover, the analysis described above indicated that the strongest binding DNA gives no stimulation or only partial stimulation of the ATPase activity. We next describe experiments that allowed us to distinguish between these alternatives.

DNA-stimulated ATPase Activity of a G-DNA Site Mutant: Evidence for Communication between the ATPase Activity and Both DNA Binding Sites—As noted above, the DNA stimulation of the ATPase activity is consistent with models in which ATP hydrolysis is not activated or partially activated upon DNA binding to one of the two DNA binding sites (Fig. 2 and supplemental Fig. S2). Fortuitously, topoisomerase II with a mutation in the G-DNA binding site has properties that allowed us to differentiate between these alternatives, as described below.

Tyrosine 782 is the nucleophilic residue that attacks DNA bound at the G-DNA binding site to give cleaved DNA and the covalent enzyme-DNA complex. Its function unambiguously identifies tyrosine 782 as within the G-DNA binding site. Mutation of this residue to phenylalanine (Y782F) prevents DNA cleavage (30) but has negligible effects on steady state ATP hydrolysis in the absence or presence of saturating DNA concentrations (Table 1). As described below, the mutation strongly alters the DNA affinities; the affinity of the higher affinity site is increased >400-fold compared with the wild-type, whereas binding of the other DNA occurs with a lower affinity. The resulting increased span between the affinities of the two DNA sites increased the ability to specifically enrich for enzyme with only one DNA bound. Thus, the ATPase activity of the complex between enzyme and only a single DNA can be more accurately determined and compared with the ATPase activities of free enzyme and enzyme saturated with DNA.

Stimulation of the ATPase activity of the Y782F enzyme is biphasic (Fig. 3 and supplemental Fig. S5). The ATPase activity of the enzyme increased 3–4-fold with DNA stoichiometric with respect to enzyme (15 nM in Fig. 3; 45 nM in supplemental Fig. S5). DNA concentrations above 1 mol eq further stimulated the ATPase activity 5–6-fold. The biphasic behavior of the DNA stimulation curve suggests that the two DNA binding sites are sequentially titrated and that each DNA that binds increases the ATPase activity. The model implies that both sites need to be occupied before ATP hydrolysis takes place at a maximal rate and that both DNA binding sites are able to signal their occupancy state to the ATPase domains. The *lines* in Fig. 3 and in supplemental Fig. S5 show a quantitative fit to this model. Using the stimulation parameters obtained from this fit and the estimated DNA affinities for the wild-type topoisomerase II (Table 2), such biphasic behavior of the stimulation

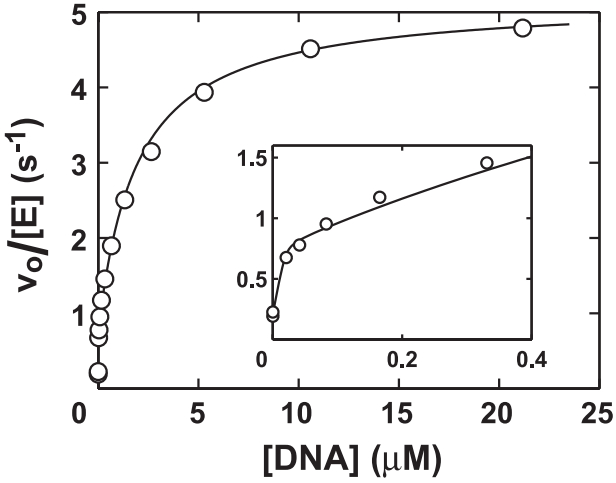

FIGURE 3. **Dependence of the observed ATP hydrolysis rate constant (v_o/[*E*]) of Y782F topoisomerase II (15 nM) on the concentration of the 68-bp DNA duplex with saturating (3 mM) Mg^{2+}-ATP.** The *line* represents a fit of the data to Scheme 1.

curves is not predicted and not observed for the wild-type enzyme at any concentration (Fig. 2*A*).

The model presented above, in which DNA bound at each site provides partial stimulation provides the simplest explanation of the data, and we further suggest that this model also holds for the wild-type enzyme, although this cannot be directly tested. More complex models cannot be ruled out. For example, we have no information about the degree of stimulation when solely the "second" DNA is bound (E_{DNA_2}), since we cannot measure the occupancy of this site. It is possible that the observed stimulation upon binding of one DNA arises from occupancy of the "second" DNA binding site by a small fraction of the DNA molecules. A large stimulation in this complex or stronger binding of the "second" DNA in the absence of the first DNA would be required for this model to hold, as described in the supplemental information. For the analysis below, we adopt the simple model of partial stimulation from DNA bound at each site.

DNA Cleavage by Topoisomerase II in the Absence of Bound T-segment DNA—The results above indicate that it is possible to prepare enzyme with a single bound DNA. We used these conditions to determine whether this lone bound DNA could be cleaved by the enzyme or whether two DNAs must be bound to allow DNA cleavage.

For the DNA cleavage experiments, we employed a 46-bp DNA duplex with a sequence that provides a high extent of cleavage to increase the experimental precision (see "Experimental Procedures"). We added increasing amounts of a ^{32}P-labeled, 46-bp DNA duplex to reaction mixtures with a constant concentration of enzyme. After allowing equilibration on the enzyme, the reaction was quenched, and the fraction of the cleaved DNA was quantified.

In the presence of the physiological divalent metal ion Mg^{2+} under conditions used in the ATPase assay described above, ~0.5–1% of the 46-bp duplex was cleaved with enzyme saturating at a concentration exceeding the DNA concentration (data not shown). Because these conditions favor binding of only one DNA per enzyme (see above), this result suggests that T-DNA

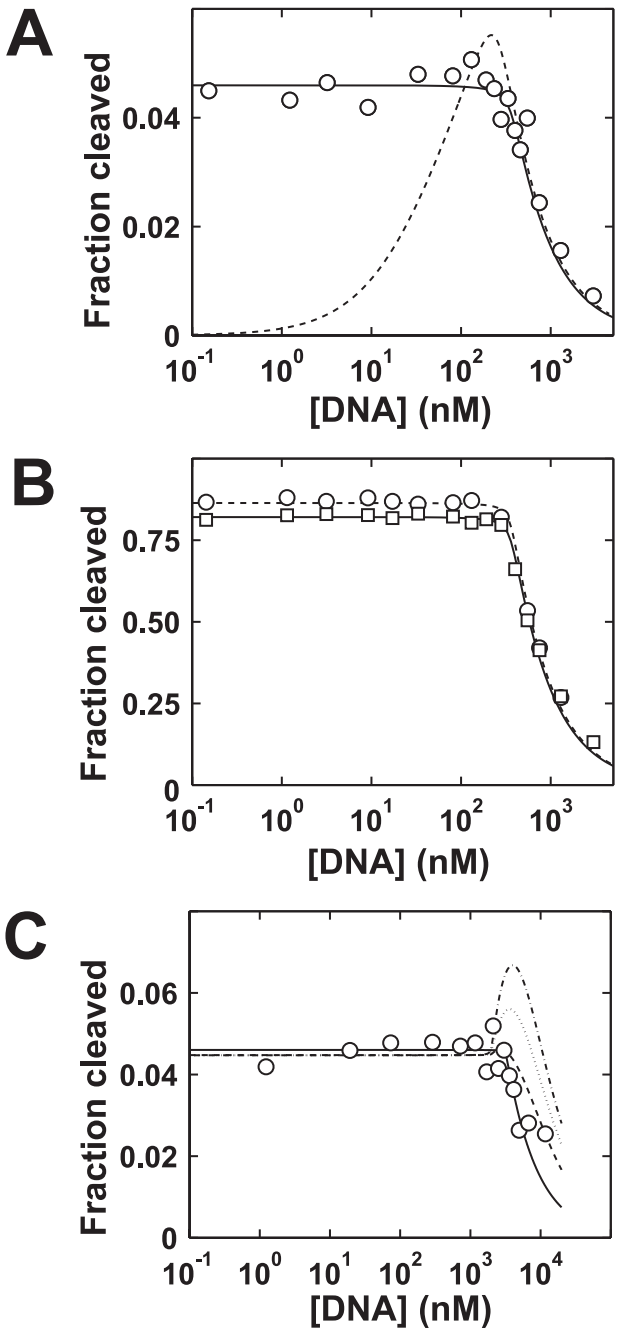

FIGURE 4. **Equilibrium DNA cleavage mediated by topoisomerase II as a function of the total concentration of a 46-bp DNA duplex (see supplemental Table S1 for sequence).** *A*, DNA titration of 360 nM topoisomerase II in the presence of 10 mM Mg^{2+} and 0.5 mM AMPPNP. Data points are averages from triplicate measurements. The data are fit to a model in which enzyme bound to a single DNA is competent to cleave DNA ($K_{clvg} > 0$; Scheme 2, *solid line*) and to a model in which T-DNA is required for DNA cleavage ($K_{clvg} = 0$; *dashed line*). As a side condition for the fits, the absence of observed DNA binding cooperativity was assumed as indicated from the analysis of the ATPase data (Table 2). Also, to demonstrate consistency of the data with a higher affinity of the G-DNA site relative to the T-DNA site, $K_d^G < K_d^T$ was used as a side condition for the fit shown by the *solid line*. *B*, DNA titrations of 360 nM topoisomerase II in the presence of 10 mM Ca^{2+} (□) or 10 mM Ca^{2+} and 0.5 mM AMPPNP (○). Lines are fits of the data to models in which K_{clvg} is allowed to exceed 0 and $K_d^G < K_d^T$, as in *A*. *C*, DNA titration of 3200 nM topoisomerase II in the presence of 10 mM Mg^{2+} and 0.5 mM AMPPNP. Data points are the averages of duplicate measurements. The *lines* are fits of the data to Scheme 2 for ratios of K'_{clvg} to K_{clvg} of 1 (*solid line*), 5 (*dashed line*), 7.5 (*dotted line*), and 10 (*dashed and dotted line*). The probability $p(\chi^2)$ that a particular model can fit the data was estimated based on a χ^2 goodness of fit test. *Solid line*, $p(\chi^2) = 0.69$; *dashed line*, $p(\chi^2) = 0.41$; *dotted line*, $p(\chi^2) = 7 \times 10^{-8}$; *dashed and dotted line*, $p(\chi^2) = 7 \times 10^{-12}$. K_d^T in AMPPNP was assumed to be 4 μM in the fits, the value obtained from DNA-stimulated ATPase activity assays using the same DNA duplex (see "Results").

is not necessary for G-DNA cleavage. However, in the presence of Mg^{2+}, only low levels of DNA cleavage can be detected (4, 31). A low signal prevents a thorough quantitative analysis, and we therefore repeated the measurement under conditions that allow higher levels of DNA cleavage.

The extent of DNA cleavage increases in the presence of ATP or ATP analogs, such as AMPPNP (4, 10, 11). Likewise, Ca^{2+} in place of Mg^{2+} has been found to stimulate topoisomerase II-mediated DNA cleavage (32) and has therefore been extensively exploited to increase the signal in DNA cleavage assays (see, for example, Refs. 4, 19, and 33). To enhance the signal to noise and allow more precise quantitation, we measured DNA cleavage in Mg^{2+} with AMPPNP, in Ca^{2+}, and in Ca^{2+} with AMPPNP. Under these conditions, DNA cleavage was also observed with enzyme in large excess relative to the DNA substrate ($>10^3$-fold; Fig. 4, *A* and *B*), conditions that according to the analysis of the ATPase data favor binding of only a single DNA per enzyme (Table 2). Cleavage under conditions that allow binding of only a single DNA is consistent with a model in which enzyme bound to only G-DNA is competent to cleave DNA. Conversely, no DNA cleavage would be expected to take place under those conditions if T-DNA binding were required for G-DNA cleavage. Further, the observed fractional DNA cleavage did not change as the DNA concentration was varied over 3 orders of magnitude, provided that the DNA concentration remained below that of the enzyme. The fraction of cleaved duplex dropped only after the DNA concentration reached approximately the enzyme concentration, as expected for a titration in which DNA binds to the G-DNA site where cleavage can occur until this site is fully titrated with DNA. As predicted by this model, the amount of DNA required to decrease the extent of cleavage in those titration curves increased linearly with increasing enzyme concentration (Fig. 4 and data not shown).

The presence of cleaved DNA with a $>10^3$-fold excess of enzyme over DNA in Mg^{2+} and Ca^{2+} and the absence of an increase in DNA cleavage with increasing DNA concentrations at DNA concentrations well below the estimated affinity of the lower affinity site (Table 2) suggests that cleavage and religation can proceed without a second bound DNA segment. The *solid lines* in Fig. 4, *A* and *C*, and the *lines* in Fig. 4*B* demonstrate that the data can be quantitatively fit by such a model, whereas a model postulating a requirement for bound T-DNA before G-DNA can be cleaved results in a poor fit to the data (Fig. 4*A*, *dashed line*). Further strong evidence against a requirement for two bound DNA molecules comes from the observation that ≥80% of the DNA duplexes were cleaved in Ca^{2+} (Fig. 4*B*), leaving at most 20% of the DNA that could, in principle, be bound at the T-DNA site. Strong evidence against alternative models is described in the supplemental information.

Human topoisomerase IIα and *E. coli* topoisomerase IV cleave DNA duplexes with DNA concentrations at least 20-fold

below the enzyme concentration (34–36). Provided that the relationships between the DNA affinities in those enzymes are similar to the yeast enzyme (*i.e.* no strong observed cooperative binding of DNA), these experimental observations suggest that these type II topoisomerases are also able to cleave DNA in the absence of a T-segment. Only for *Drosophila* topoisomerase II was cleavage not detected with substoichiometric DNA (19). The *Drosophila* enzyme may possess properties that differ from those of other type II topoisomerases in terms of the relative affinities of the DNA binding sites or the communication between the sites. In summary, these results provide strong evidence that a single DNA bound at the G-site of yeast topoisomerase II can be cleaved.

The Relative Affinities of DNA for the G and T Binding Sites—The ATPase assay provided thermodynamic information about two DNA binding sites and suggested that one binding site can be enriched with DNA. The presence of DNA cleavage under conditions where only one DNA is bound can be most simply explained if the DNA that is cleaved (G-DNA) binds more strongly than the DNA that is transported (T-DNA; $K_d^G < K_d^T$; Scheme 2 and Fig. 4). Cleavage under those conditions, however, does not rule out the possibility that the affinity of the T-DNA site could be greater than that of the G-DNA site ($K_d^T < K_d^G$). Exhaustive quantitative modeling indicated that the DNA cleavage data can be fit by this alternative model but only if binding of the T-segment to enzyme with DNA bound at the G-DNA site decreases the cleavage equilibrium at the G-DNA binding site ($K'_{clvg} \leq K_{clvg}$; supplemental Fig. S6). A reduced cleavage equilibrium in the presence of T-DNA is possible but is mechanistically unexpected (25, 37).

The effect of the site-specific mutation in the G-DNA site (Y782F) on binding of DNA to both binding sites provides additional information to distinguish between binding at the G-DNA and T-DNA binding sites. The affinity of the highest affinity binding site can be isolated using a DNA binding assay in which the enzyme is kept in excess of DNA. We measured equilibrium DNA binding with wild-type and mutant enzyme under standard assay conditions using a fluorescence polarization anisotropy assay. Trace amounts of fluorescently labeled DNA were allowed to bind to varying concentrations of topoisomerase II. Complex formation between DNA and enzyme was monitored by the resulting increase in the fluorescence anisotropy (Fig. 5). Compared with the wild-type enzyme, the Y782F mutant bound DNA >400-fold more tightly. Although a previous report suggested similar binding of DNA to wild-type and Y782F topoisomerase II in a low ionic strength buffer (18), it is likely that enzyme aggregation and tight binding prevented accurate determination of these dissociation constants under those conditions (see "Experimental Procedures" and supplemental Fig. S7).

An estimate of the DNA affinity for binding a second DNA can be obtained from the DNA stimulation curves of the ATPase activity, since the ATPase assay is most sensitive to the fraction of enzyme bound to two DNAs. About 10-fold higher DNA concentrations were necessary to half-maximally stimulate the ATPase activity of the Y782F mutant compared with wild type under similar conditions (Figs. 2 and 3), suggesting that binding of the second DNA occurs with ~10-fold weaker

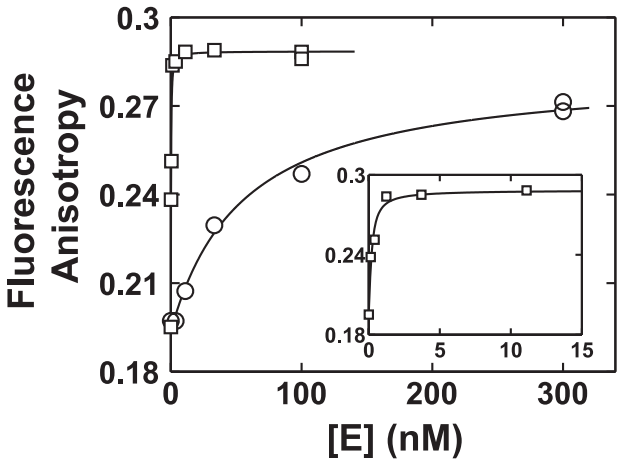

FIGURE 5. **Equilibrium fluorescence anisotropy measurement of wild-type and Y782F mutant topoisomerase II to a fluorescently labeled 40-bp DNA duplex (see supplemental Table S1 for sequence).** The indicated concentrations of wild-type (○) and Y782F mutant (□) enzyme were used to titrate 0.8 and 0.16 nM DNA, respectively. Fitting the data to quadratic binding isotherms (Equation 2; *lines*) gave apparent binding affinities for the wild-type and mutant enzymes of $K_{d,\ wild\ type} = 60$ nM and $K_{d,\ Y782F} \leq 0.14$ nM, respectively. The apparent DNA affinity for the mutant enzyme is an upper limit, because the DNA concentration employed in this experiment (0.16 nM) is similar to the apparent affinity.

DNA affinity. Quantitative analysis of the ATPase data confirms this conclusion (Table 2, $K_d^{2'}$).

The simplest interpretation of these data is that the larger (>400-fold) effect of the Y782F mutation on DNA binding to the higher affinity site is derived from a local perturbation of DNA binding rather than from an indirect effect. Correspondingly, the smaller (10–30-fold) effect on the weaker affinity site would arise from an indirect, longer range effect of the mutation. Although this assignment is not proven by the data herein, it provides the simplest, self-consistent explanation for multiple experimental results.

Does Binding of a T-segment DNA Affect DNA Cleavage at the G-DNA Site?—The results described above strongly suggest that DNA bound at the G-DNA site can be cleaved without DNA bound at the T-DNA site. Here we ask whether occupancy of the T-DNA site alters the cleavage equilibrium. The weakened T-segment affinity in the mutant that has an amino acid change in the G-DNA site (Y782F) compared with wild type indicates that there can be communication between the G-DNA site and the T-DNA site. Positive coupling between T-DNA binding and G-DNA cleavage has been proposed. Crystal structures of isolated ATPase domains reveal a cavity between the dimerized subunits that is too small to comfortably accommodate double-stranded DNA (see Ref. 38 and references therein). For that reason, it has been suggested that closure of the ATPase domains around a T-segment leads to strain in the ATPase domains that may promote DNA cleavage ($K'_{clvg} > K_{clvg}$; Scheme 2) (37). In a report on DNA gyrase, it was noted that excess DNA, presumably acting as a T-segment, had a stimulatory effect on DNA cleavage (25).

If T-DNA binding enhances DNA cleavage, a higher fraction of cleavage would be expected once all available G-DNA sites have been titrated with DNA and additional DNA has bound to the T-DNA site. We therefore repeated the DNA titration experiment in Mg^{2+}-AMPPNP shown in Fig. 4*A* with a 1-order

of magnitude higher enzyme concentration (3.2 μM; Fig. 4*C*), so that DNA added in excess of the G-DNA sites would bind to the T-DNA sites of the enzyme (K_M^{duplex} in the ATPase assay provides an estimate for the affinity of the second DNA; $K_M^{46\ \text{bp}} = 2.7\ \mu$M and $K_M^{46\ \text{bp}} = 4\ \mu$M with saturating and subsaturating ATP concentrations, respectively (data not shown)). The resulting titration curve shown in Fig. 4*C* has a shape indistinguishable from the one with lower enzyme concentration (0.36 μM; Fig. 4*A*). Both titration curves can be fit by a model in which the cleavage equilibrium is unaltered by T-DNA binding ($K'_{\text{clvg}} = K_{\text{clvg}}$; *solid lines*). The data therefore provide no evidence for an effect of T-DNA on DNA cleavage. Assuming that the T-DNA affinity is not significantly weakened with AMPPNP instead of ATP present, a conservative upper limit of 10-fold stimulation of DNA cleavage by the T-DNA (with bound AMPPNP) is established (Fig. 4*C*).

DISCUSSION

Type II topoisomerases and other molecular machines couple chemical energy to physical work. In the case of type II topoisomerases, one DNA duplex is transported through a transient break in another strand in a reaction that is coupled to the expenditure of ATP (4). Although substantial biochemical and structural information on the overall reaction cycle of topoisomerase II is available (see Fig. 1 and Introduction) the biochemical and structural basis for coupling ATP hydrolysis to DNA transport is incompletely understood. A critical step in unraveling the intramolecular communication responsible for coupling is to physically or temporally isolate different reaction complexes and intermediates to allow the behavior of each of these species to be followed and dissected. Since topoisomerase II contains at least two DNA binding sites, one for the DNA undergoing transport (T-DNA site) and one for the DNA through which this helix is transported (G-DNA site) (6, 14, 28, 29), it is imperative to distinguish the effects and behavior of DNA bound at each of these sites.

The data herein indicate that it is possible to enrich enzyme bound to a single DNA using short DNA duplexes that are long enough to bind strongly but not long enough to simultaneously contact both binding sites. The results strongly suggest that DNA binds preferentially to the G-DNA site and that there is at most limited cooperativity in the overall binding of the two DNAs.

The ability to enrich enzyme with DNA bound at the G-site provided the opportunity to directly test if the presence of the T-segment is allosterically required for DNA cleavage at the G-site. Cleavage and religation can proceed without DNA bound at the T-DNA site (Fig. 4), providing strong evidence against the model that T-DNA binding is required before G-DNA cleavage takes place (19). Binding of nucleotide (AMPPNP) to the ATPase domains stimulated DNA cleavage in the absence of a T-segment (Fig. 4 and data not shown). Thus, the ATPase domains are able to communicate with the G-DNA site and do so in the absence of DNA occupying the T-DNA site. Nevertheless, the observed change in binding affinity of DNA at the T-DNA site from a point mutation in the G-DNA site (Y782F) indicates that there is communication between these sites, and it remains possible that there is a modest amount of coupling between T-DNA binding and DNA cleavage (see "Results"). The >400-fold increase in the DNA affinity at the G-DNA site from the mutation of the tyrosine residue that serves as the nucleophile in DNA cleavage may reflect ground state destabilization in the wild-type enzyme that is used to facilitate DNA cleavage or formation of the conformational state needed to accomplish overall DNA transport.

That the presence of DNA stimulates ATP turnover by topoisomerase II has been known for decades (12), but the molecular mechanism for this stimulation has remained elusive. A dissection of this mechanism requires knowledge of which DNA binding site communicates with the ATPase reaction, and prior results have been interpreted in favor of either the G- or the T-DNA binding site (see Introduction). Based on results obtained with the Y782F mutant and wild-type enzyme, we conclude that neither binding site alone is sufficient for the full stimulation potential of DNA. Binding of G-DNA partially activates ATP hydrolysis, and binding of T-DNA at higher concentrations of DNA completes the activation. The presence of communication between both DNA binding sites and the ATPase activity is presumably a manifestation of the cooperative enzyme environment in topoisomerase II, a molecular machine that relies on intramolecular communication to couple chemical and physical reaction steps.

Closure of the ATPase domains has been implicated as a conformational change that precedes ATP hydrolysis, and the x-ray crystal structures of ATPase fragments reveal contacts between the ATPase domains of the two subunits in regions that form the ATP binding site (2, 7, 8, 15–17). ATPase domains created by truncation of topoisomerase II dimerized in the presence of DNA, suggesting a role of DNA binding in facilitating domain closure (16). The stimulation of ATP hydrolysis by binding of each DNA observed herein suggests that this domain closure may be coupled to both the T-DNA and the G-DNA binding.

This work not only provides insights into intramolecular communication of a complex molecular machine but also builds the foundation for in depth mechanistic dissections of the working mechanism of topoisomerase II. Because DNA cleavage can proceed without the presence of a T-DNA, simplified reaction conditions that only allow G-DNA to bind can be used in future studies to isolate and mechanistically dissect G-DNA binding and cleavage and to analyze the mechanism of cross-talk between the DNA cleavage and ATPase domains.

Acknowledgments—We thank Janet Lindsley (University of Utah) for kindly providing topoisomerase II expression plasmids, the yeast strain BCY123, and helpful discussions, Zeynep Oekten for help with the purification of the Y782F mutant enzyme, and the Herschlag laboratory for critically reading the manuscript.

REFERENCES

1. Wang, J. C. (1996) *Annu. Rev. Biochem.* **65,** 635–692
2. Corbett, K. D., and Berger, J. M. (2004) *Annu. Rev. Biophys. Biomol. Struct.* **33,** 95–118
3. Schoeffler, A. J., and Berger, J. M. (2005) *Biochem. Soc. Trans.* **33,** 1465–1470

4. Lindsley, J. E., and Wang, J. C. (1993) *J. Biol. Chem.* **268,** 8096–8104
5. Baird, C. L., Harkins, T. T., Morris, S. K., and Lindsley, J. E. (1999) *Proc. Natl. Acad. Sci. U. S. A.* **96,** 13685–13690
6. Roca, J., and Wang, J. C. (1992) *Cell* **71,** 833–840
7. Ali, J. A., Jackson, A. P., Howells, A. J., and Maxwell, A. (1993) *Biochemistry* **32,** 2717–2724
8. Hu, T., Sage, H., and Hsieh, T. S. (2002) *J. Biol. Chem.* **277,** 5944–5951
9. Wigley, D. B., Davies, G. J., Dodson, E. J., Maxwell, A., and Dodson, G. (1991) *Nature* **351,** 624–629
10. Sander, M., and Hsieh, T. (1983) *J. Biol. Chem.* **258,** 8421–8428
11. Osheroff, N. (1986) *J. Biol. Chem.* **261,** 9944–9950
12. Liu, L. F., Liu, C. C., and Alberts, B. M. (1979) *Nature* **281,** 456–461
13. Osheroff, N., Shelton, E. R., and Brutlag, D. L. (1983) *J. Biol. Chem.* **258,** 9536–9543
14. Tingey, A. P., and Maxwell, A. (1996) *Nucleic Acids Res.* **24,** 4868–4873
15. Gardiner, L. P., Roper, D. I., Hammonds, T. R., and Maxwell, A. (1998) *Biochemistry* **37,** 16997–17004
16. Olland, S., and Wang, J. C. (1999) *J. Biol. Chem.* **274,** 21688–21694
17. Campbell, S., and Maxwell, A. (2002) *J. Mol. Biol.* **320,** 171–188
18. Morris, S. K., Harkins, T. T., Tennyson, R. B., and Lindsley, J. E. (1999) *J. Biol. Chem.* **274,** 3446–3452
19. Corbett, A. H., Zechiedrich, E. L., and Osheroff, N. (1992) *J. Biol. Chem.* **267,** 683–686
20. Kallansrud, G., and Ward, B. (1996) *Anal. Biochem.* **236,** 134–138
21. Gill, S. C., and von Hippel, P. H. (1989) *Anal. Biochem.* **182,** 319–326
22. Lindsley, J. E. (2001) *Methods Mol. Biol.* **95,** 57–64
23. Horst, M., Oppliger, W., Feifel, B., Schatz, G., and Glick, B. S. (1996) *Protein Sci.* **5,** 759–767
24. Kraut, D. A., Sigala, P. A., Pybus, B., Liu, C. W., Ringe, D., Petsko, G. A., and Herschlag, D. (2006) *PLoS Biol.* **4,** e99
25. Kampranis, S. C., Bates, A. D., and Maxwell, A. (1999) *Proc. Natl. Acad. Sci. U. S. A.* **96,** 8414–8419
26. Wang, J. C. (1998) *Q. Rev. Biophys.* **31,** 107–144
27. Maxwell, A., and Gellert, M. (1984) *J. Biol. Chem.* **259,** 14472–14480
28. Roca, J., Berger, J. M., and Wang, J. C. (1993) *J. Biol. Chem.* **268,** 14250–14255
29. Berger, J. M., Gamblin, S. J., Harrison, S. C., and Wang, J. C. (1996) *Nature* **379,** 225–232
30. Liu, Q., and Wang, J. C. (1998) *J. Biol. Chem.* **273,** 20252–20260
31. Burden, D. A., Froelich-Ammon, S. J., and Osheroff, N. (2001) *Methods Mol. Biol.* **95,** 283–289
32. Osheroff, N., and Zechiedrich, E. L. (1987) *Biochemistry* **26,** 4303–4309
33. Strumberg, D., Nitiss, J. L., Dong, J., Walker, J., Nicklaus, M. C., Kohn, K. W., Heddle, J. G., Maxwell, A., Seeber, S., and Pommier, Y. (2002) *Antimicrob. Agents Chemother.* **46,** 2735–2746
34. Bromberg, K. D., Burgin, A. B., and Osheroff, N. (2003) *Biochemistry* **42,** 3393–3398
35. Bromberg, K. D., Burgin, A. B., and Osheroff, N. (2003) *J. Biol. Chem.* **278,** 7406–7412
36. Marians, K. J., and Hiasa, H. (1997) *J. Biol. Chem.* **272,** 9401–9409
37. Classen, S., Olland, S., and Berger, J. M. (2003) *Proc. Natl. Acad. Sci. U. S. A.* **100,** 10629–10634
38. Corbett, K. D., and Berger, J. M. (2005) *Structure* **13,** 873–882

Supplementary Methods

Enzyme expression and purification

The expression vector pJEL236 (18) encoding the full length *S. cerevisiae* topoisomerase II enzyme fused to an intein and a chitin binding domain was kindly provided by Janet Lindsley, University of Utah. A secondary mutation (A3925G) was reverted to the wild-type sequence by QuickChange site directed mutagenesis (Stratagene) after subcloning the coding sequence into pBluescript II KS+ (Fermentas). In addition, a Y782F mutation was introduced by QuickChange mutagenesis. The coding sequences were cloned back into the pJEL236 vector backbone. A kanamycin resistence gene was inserted into the Apa1 site to yield pFMP54 encoding wild-type and pFMP69 encoding the Y782F mutant topoisomerase. The DNA sequences were verified by DNA sequencing of the full coding regions. The constructs were designed such that the only difference between *S. cerevisiae* topoisomerase II and the final, purified topoisomerase is a change of the C-terminal aspartic acid is to glycine. Purified protein with this one change was reported to have identical biochemical characteristics to the fully wild-type enzyme (18); for the purposes of these studies, it is referred to as wild-type topoisomerase II.

Single colonies of the yeast expression strain BCY123 harboring pFMP54 or pFMP69 were grown in YP-Raffinose in the presence of 0.2 mg/mL G418 (A.G. Scientific). Cells were induced and harvested as described (18) and stored at -80 ˚C. To purify topoisomerase II, cells were lysed in liquid nitrogen using a Waring blender. Chitin affinity chromatography was performed essentially as described (18). Intein cleavage was induced with 30 mM DL-dithiothreitol (Sigma) overnight at 4 ˚C in FPLC buffer [50 mM potassium HEPES pH 7.5, 20% sucrose, 0.1 mM EDTA, 0.01% Tween 20] plus 500 mM potassium acetate (KOAc). Protein containing fractions from the elution were diluted 1:1 with FPLC buffer + 100 mM KOAc and loaded on a Heparin FF column (Pharmacia) from which topoisomerase II was eluted with a KOAc gradient (0.25 to 0.7 M). Topoisomerase-containing fractions were loaded undiluted on a MonoQ (Pharmacia) column and eluted with a KOAc gradient (0.5 to 1 M). The most concentrated fractions were pooled and further concentrated to 10-30 μM using an Amicon Ultra (Millipore) 100K cutoff centrifugal filter. The concentrate was aliquoted and stored at -80 ˚C. Per 40 g of wet weight cells (from ~8 L culture), the yield was 5 mg for wild-type and 1 mg for Y782F topoisomerase II. The purity was ≥95% based on Coomassie Blue staining of SDS gels (Supplementary Figure S1 and data not shown). Topoisomerase II can be reversibly phosphorylated. The phosphorylation state of the enzyme was not monitored or controlled.

Selection of the DNA duplex for the DNA cleavage assay

Topoisomerase-mediated cleavage of the 40 bp and 68 bp duplex substoichiometric with respect to enzyme in the presence of Mg^{2+}-AMPPNP could be detected, but the signal was too low for accurate quantification (<1%; data not shown). A series of duplexes with palindromic sequences was created based on the cleavage site within the 40 bp duplex (unpublished results). The lengths of these duplexes were increased to 46 bp to position the cleavage site in the center of the DNA. The sequence providing the highest extent of cleavage was selected for the cleavage experiments herein (Supplementary Table S1). The cleavage specificity of the main cleavage site of the 46 bp duplex used in this study was >95% (data not shown).

ATPase assay

ATP hydrolysis was measured by a coupled ATPase assay using pyruvate kinase (15 U/mL final concentration), PEP (6 mM), lactate dehydrogenase (15 U/mL), NADH (0.5 mM) and varying concentrations of Mg^{2+}-ATP in 0.1 mL reactions. The absorption of NADH over time was read by a SpectraMax 340 PC 96 well plate reader in flat bottom, uncoated 96 well plates (Nunc). ATP resynthesis apparently did not limit the measured rates: varying the ATP regenerating system concentration two-fold did not result in changes of the measured rates. This result is corroborated by control experiments in which the solution containing the ATP regenerating system was mixed with pure ADP. Rates for ATP regeneration in those experiments were at least five times faster that the rates in experiments containing topoisomerase II. Individual ATPase activities between independent experiments varied on average 7% (standard error) for saturating (3 mM) and 15% for subsaturating (0.06 mM) ATP concentrations.

Supplementary Results

Models to account for the biphasic DNA stimulation of the ATPase activity of the Y782F topoisomerase II

Three limiting models can account for the observed biphasic DNA stimulation curve of the Y782F enzyme (Supplementary Scheme 3). The first model was presented in the main text and is shown in the Supplementary Scheme 3A for comparison. According to this model, binding of DNA to the higher affinity binding site (defined as K_d^1; the thickness of the red arrows indicates the relative affinities of different enzyme species for DNA) partially stimulates ATP hydrolysis. Increased ATP hydrolysis is indicated by thicker, blue arrows in Supplementary Scheme 3. This model implies communication between each DNA binding site and the ATPase activity, as binding of each DNA activates ATP hydrolysis. The modest level of stimulation observed from binding of the first DNA to the mutant enzyme would not be expected to be detectable in the analogous experiment with the wild-type enzyme, as the affinities for the first and second DNAs are not sufficiently different in the wild-type. Thus, the results with the wild-type enzyme do not provide evidence for this model but are fully consistent with it (Supplementary Figure S2).

A second model to explain the biphasic stimulation curve does not require that DNA bound at the higher affinity site partially activates ATP hydrolysis. The ATPase activity is stimulated only in complexes that have the lower affinity site occupied (E_{DNA_2} and $E_{DNA_2}^{DNA_1}$; Supplementary Scheme 3B). To obtain measurable ATPase stimulation by binding of a single DNA in this model, a significant fraction of DNA would have to be bound to the lower affinity site under conditions when the enzyme is in excess of DNA (i.e. $K_d^1 \sim K_d^2$). The dissociation constant for the second DNA to bind to the mutant enzyme is significantly larger than that for the first DNA [$K_d^1 < 1$ nM (Scheme 1), $K_d^{2'} \geq 550$ nM (Table II) and data not shown]. Consequently, the model requires that DNA binding exhibits negative binding cooperativity ($K_d^2 < K_d^{2'}$): i.e., G-DNA binding would inhibit binding of T-DNA and vice versa. However, negative binding cooperativity of more than three-fold is not consistent with ATPase activity results for the wild-type enzyme under identical conditions (Supplementary Figure Supplementary Figure S3C). Thus, the Y782F mutation would have to induce negative DNA binding cooperativity not present in the wild-type enzyme for this model to hold.

A third model requires that the enzyme species with DNA bound only at the lower affinity site (E_{DNA_2}) have a hyperstimulated ATPase activity compared to the other enzyme species (Supplementary Scheme 3C). Even though E_{DNA_2} cannot strongly accumulate in this model due to unfavorable DNA affinities ($K_d^1 << K_d^2$) , the small fraction of E_{DNA_2} formed with enzyme in excess of DNA would be sufficient to significantly stimulate the observed ATPase activity. Quantitative analysis shows that the ATPase activity of E_{DNA_2} would have to be stimulated >1000-fold compared to free enzyme to fit the data (analysis not shown). Because the overall DNA stimulation of the ATPase activity at saturating DNA concentrations is only ~20-fold compared to DNA free enzyme, binding of the second DNA segment would then have to inhibit DNA stimulation by at least 50-fold. As in the first model described above, this model requires communication between both DNA binding sites and the ATPase activity except that in this model DNA_2 in the $E_{DNA_2}^{DNA_1}$ -complex is stimulatory and DNA_1 is inhibitory to the ATPase activity. This model, like the first, is consistent with data obtained with the wild-type enzyme (data not shown).

In summary, models 1 and 3 require that both DNA binding sites can communicate with the ATPase domains. While in model 1 each DNA partially activates ATP hydrolysis, model 3 postulates one inhibitory and one stimulatory binding site. In contrast, model 2 demands that only one of the DNA binding sites is stimulatory to the ATPase activity. Model 2 requires that the Y782F mutation induces negative DNA binding cooperativity between the two binding sites, and model 3 requires that a hyperstimulated ATPase state exists. We adopt the first model (Supplementary Scheme 3A) as our working model due to its simplicity, its consistency with the DNA-dependent ATPase stimulation for the wild-type enzyme, and the lack of a requirement for additional *ad hoc* assumptions.

Alternative models accounting for the DNA dependence of DNA cleavage

As described in the main text, the DNA dependence of DNA cleavage is consistent with a model that does not require the presence of a bound T-segment before the G-segment can be cleaved. Two alternative models could in principle also account for the data, but they can be rejected based on data presented herein and additional unpublished results, as described below.

First, DNA binding could be strongly cooperative, such that under the conditions employed the enzyme would never be significantly bound to only a single DNA (Supplementary Scheme 4; thickness of arrows indicates the relative affinities). In this case, it would not be

possible to distinguish if the T-segment were required allosterically for cleavage. However, at most 50% of the DNA could be cleaved in this scenario because at most 50% of the DNA segments could be bound at the G-DNA site. Thus, this model could only explain the DNA cleavage data obtained in Mg^{2+} where <10% cleavage is observed, but is not consistent with the >80% DNA cleavage observed in Ca^{2+}. A quantitative analysis of the data showed that binding of the second segment in Mg^{2+} would have to occur with a $\geq 10^4$-fold higher affinity than binding of the first ($K_d^{T'} \leq K_d^G / 10^4$ and $K_d^{G'} \leq K_d^T / 10^4$, i.e., with 10^4-fold observed binding cooperativity; Supplementary Figure S6 and data not shown). However, the analysis of the dependence of ATPase hydrolysis on the concentration of the 40 bp and 68 bp duplexes indicates that there is no observed binding cooperativity (Table II). Differences between the DNA cleavage assay conditions compared to the ATPase assay conditions are not responsible for inducing observed cooperativity*. Thus, a model requiring strong, positive observed cooperativity to explain the DNA cleavage results can be rejected.

In a second alternative model, DNA could bind transiently at the T-DNA binding site and induce cleavage of a bound G-DNA. The DNA at the T-DNA site could then dissociate and bind to the T-DNA site of another enzyme molecule promoting cleavage and so forth. This possibility can be ruled out based on unpublished kinetic results, as follows. Microscopic reversibility would require that T-DNA also be required for ligation of cleaved DNA at the G-DNA site. However, DNA religation by topoisomerase II followed in pulse-chase type experiments in which ligation is induced by adding in a large excess of unlabeled DNA or by diluting the reaction mixture give the same rate constant for ligation (unpublished results). These results indicate that a second, transiently bound DNA is not involved in establishing the cleavage/ligation equilibrium.

*A 46 bp duplex was employed in the DNA cleavage assay while a 40 bp and a 68 bp duplex were used in the ATPase assay opening the possibility that the specific length or sequence of the 46 bp duplex could promote observed binding cooperativity. The observation of DNA cleavage in Mg^{2+}, Mg^{2+}-AMPPNP, Ca^{2+} and Ca^{2+}-AMPPNP for the 40 bp and 68 bp DNA duplexes under conditions where the enzyme was in large excess of DNA provides evidence against that possibility (data not shown). Furthermore, it is possible that AMPPPNP used in the DNA cleavage assay induces observed binding cooperativity. Evidence against that possibility comes from the observation that DNA cleavage of the 40 bp, 46 bp and 68 bp duplexes was detected also in the absence of AMPPNP in Mg^{2+} with the enzyme concentration in large excess of the DNA concentration (data not shown). Finally, the presence of bound ATP in the ATPase assay may prevent observed DNA binding cooperativity. However, the analysis of the ATPase data indicated the absence of observed DNA binding cooperativity also under subsaturating ATP conditions (Table II).

Table S1 Oligodeoxyribonucleotides used in this study

Name	**Sequence (5' – 3')**
$Oligo_{68}$top	GCTAACGCAGTCAGGCACCGTGTATGAAATCTAACAATGCGCTCATCGTCATCCTCGGCACCGTCACC
$Oligo_{68}$bottom	GGTGACGGTGCCGAGGATGACGATGAGCGCATTGTTAGATTTCATACACGGTGCCTGACTGCGTTAGC
$Oligo_{40}$top	TGAAATCTAACAATGCGCTCATCGTCATCCTCGGCACCGT
$Oligo_{40}$bottom	ACGGTGCCGAGGATGACGATGAGCGCATTGTTAGATTTCA
$Oligo_{40}$top-ROX [a]	ROX-TGAAATCTAACAATGCGCTCATCGTCATCCTCGGCACCGT
$Oligo_{46}$ [b]	ACGGTGCCGAGGATGACGATGCGCGCATCGTCATCCTCGGCACCGT

[a] ROX: 6-Carboxy-X-rhodamine.

[b] $Oligo_{46}$ is self-complementary, so top and bottom strands are identical.

Supplementary Scheme 3

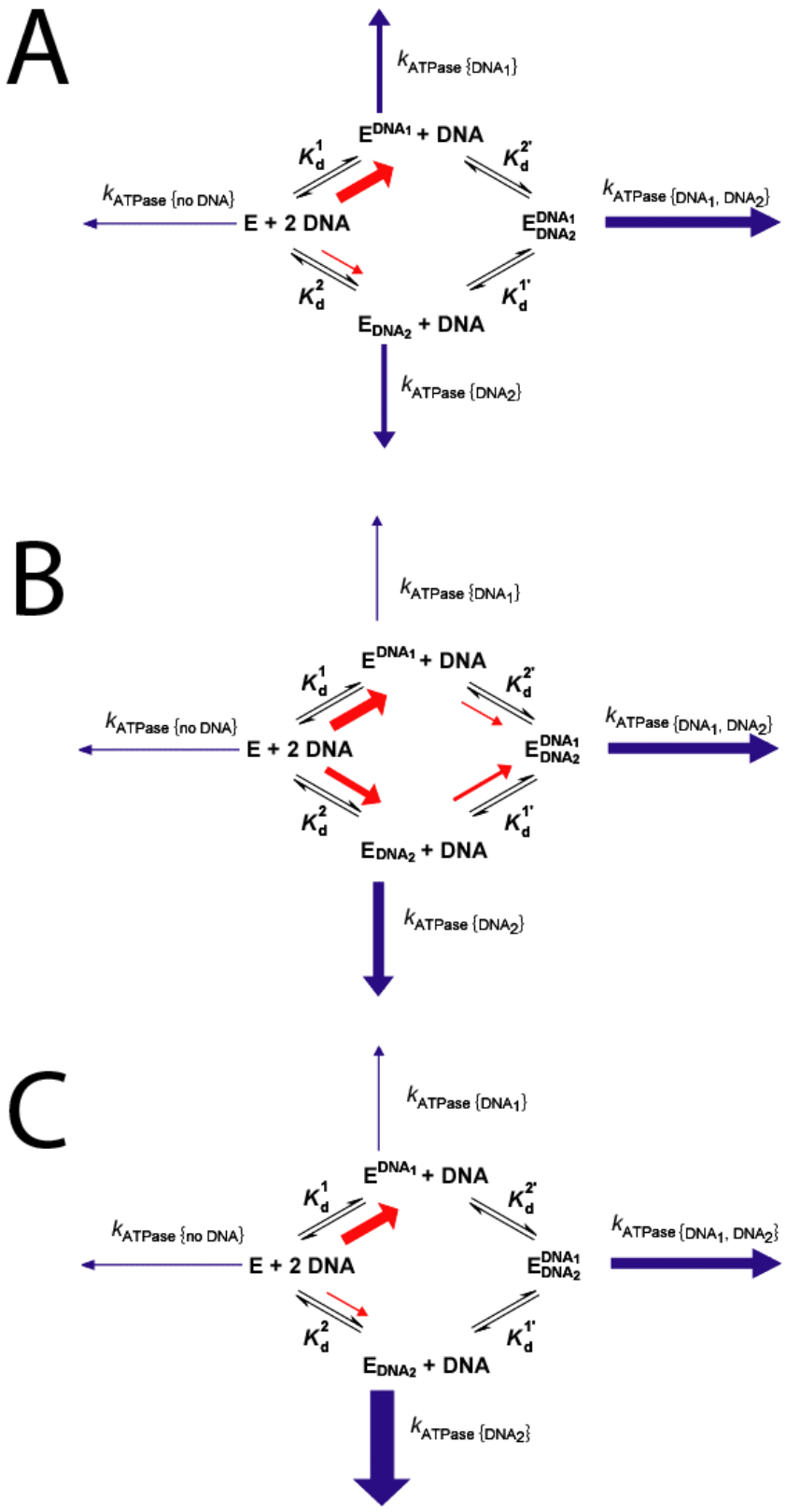

Supplementary Scheme 4

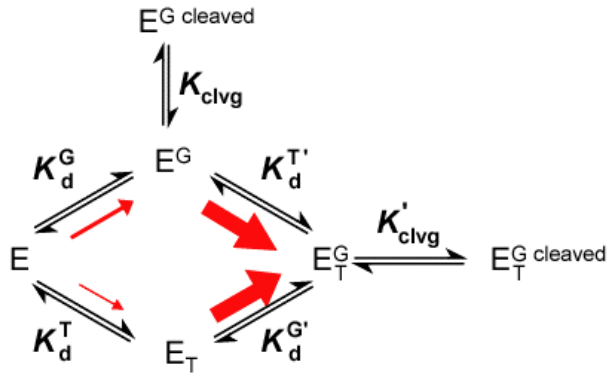

Supplementary Figures

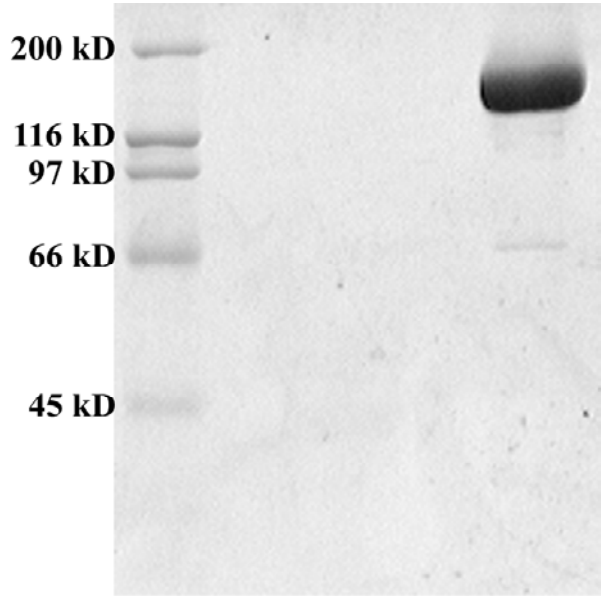

Supplementary Figure S1: Assessment of the purity of the topoisomerase II preparation. Purified wild-type topoisomerase II (~1 μg; theoretical molecular weight 164 kD) was analyzed on a 10% SDS polyacrylamide gel and stained with Coomassie Blue. Quantification of bands in the gel indicates a purity of ≥95% of the topoisomerase II preparation.

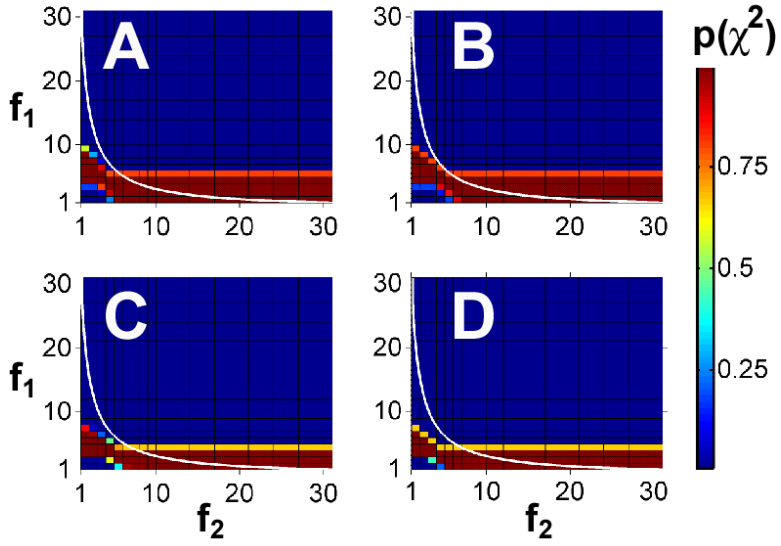

Supplementary Figure S2: Range of ATPase stimulation that can be elicited by each bound DNA segment in the absence of the other. The DNA stimulation curves of the ATPase activity at saturating ATP concentrations from Figure 2A were fit to a set of models with ATPase activities for E and $E_{DNA_2}^{DNA_1}$ fixed at the levels observed in the absence of DNA and the presence of saturating DNA, respectively, but varied in the level of the ATPase activity for E^{DNA_1} and E_{DNA_2} (Scheme 1). The ratio between the ATPase activity of E^{DNA_1} and E is defined as f_1, and f_2 is similarly defined as the ratio of the ATPase activities of E_{DNA_2} and E. The probability $p(\chi^2)$ that a particular model can fit the data was estimated based on a chi square goodness-of-fit test. K_d^2 in the fits is defined to be of equal or greater value than K_d^1 ($K_d^2 \geq K_d^1$) as it refers to the weaker binding site. $p(\chi^2)$ is plotted over a plane defined by f_1 and f_2. Different ranges of values for $p(\chi^2)$ are assigned different colors. Models with a low probability to fit the data based on the χ^2 test are assigned a blue color (see color bar). To fit the data, K_M^{ATP} values for all four enzyme species are needed (see Experimental Procedures), but only the K_M^{ATP} values for free enzyme (E, $K_{M\{\text{no DNA}\}}^{ATP} = 1$ mM) and $E_{DNA_2}^{DNA_1}$ ($K_{M\{DNA_1,DNA_2\}}^{ATP} = 0.2$ mM; Table I) are known. Four permutations of K_M^{ATP} values of E^{DNA_1} and E_{DNA_2} that span the values for E and $E_{DNA_2}^{DNA_1}$ were considered: A) $K_{M\{DNA_1\}}^{ATP} = K_{M\{DNA_2\}}^{ATP} = 1$ mM. B) $K_{M\{DNA_1\}}^{ATP} = 1$ mM and $K_{M\{DNA_2\}}^{ATP} = 0.2$ mM. C) $K_{M\{DNA_1\}}^{ATP} = 0.2$ mM and $K_{M\{DNA_2\}}^{ATP} = 1$ mM. D) $K_{M\{DNA_1\}}^{ATP} = K_{M\{DNA_2\}}^{ATP} = 0.2$ mM. Values for

$K_{M\{DNA_1\}}^{ATP}$ and $K_{M\{DNA_2\}}^{ATP}$ below 0.2 mM or above 1 mM are possible. K_M^{ATP} values below 0.2 mM would not change the conclusions because ATP remains saturating for all species. Values significantly above 1 mM would prevent ATP from being saturating for the particular species; the ATPase activity of this species would still be stimulated by DNA but the reported stimulation would be an underestimate. The white line indicates the position of models for which the product of f_1 and f_2 totals the maximal stimulation observed at saturating DNA concentrations of 31-fold.

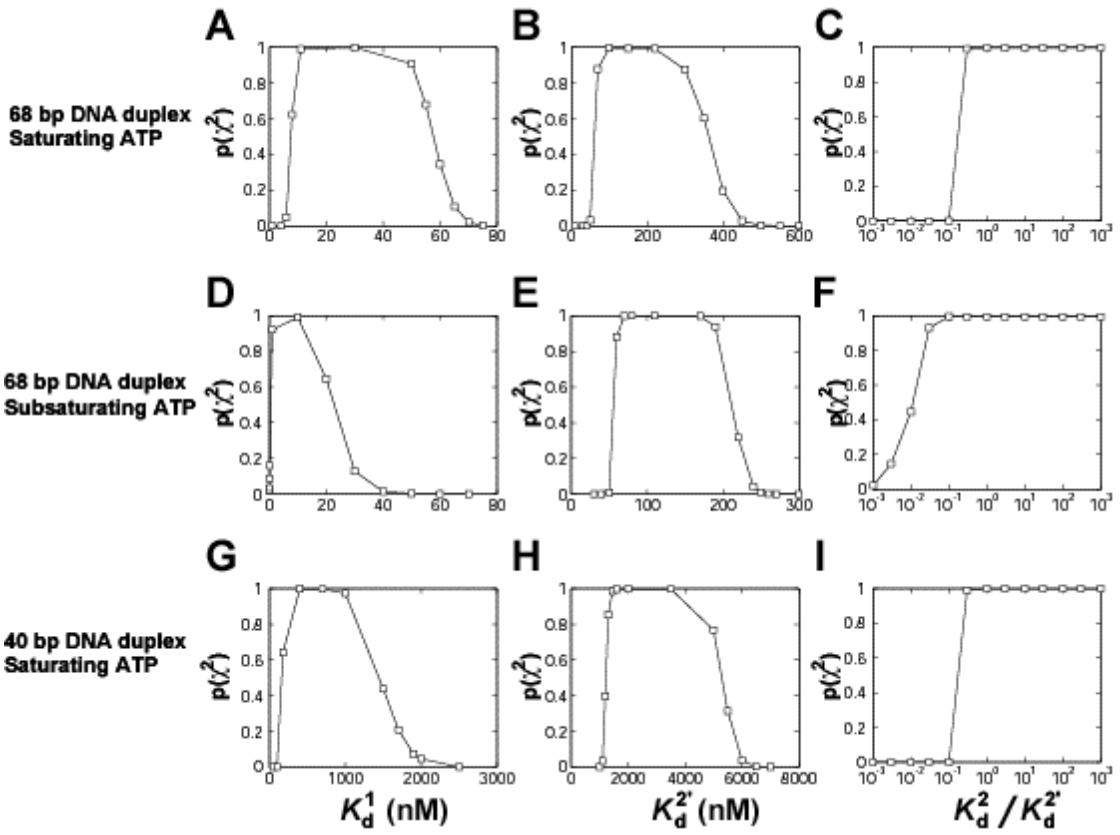

Supplementary Figure S3: Estimation of limits for K_d^1, $K_d^{2'}$ and $K_d^2 / K_d^{2'}$ (Scheme 1) for wild-type enzyme obtained from the DNA stimulation of the ATPase activity in Figure 2 and Supplementary Figure S4. The DNA stimulation curves of the ATPase activity using a 68 bp duplex under saturating (panels A, B and C), and subsaturating ATP concentrations (panels D, E and F) and the DNA stimulation curves using a 40 bp duplex under saturating ATP concentrations (panels G, H and I) were fit to models that systematically varied the indicated parameters, and the goodness of the fit for each model was estimated based on a χ^2 goodness-of-fits test. Values for the indicated parameters that give $p(\chi^2) \geq 0.05$ were considered acceptable and are summarized in Table II. In panels A, D and G, K_d^1 was systematically varied. $K_d^{2'}$ was varied in panels B, E, and H, and the degree of DNA binding cooperativity ($K_d^2 / K_d^{2'}$) was varied in panels C, F, and I. Partial ATPase stimulation of E^{DNA_1} and E_{DNA_2} compared to E was allowed in the fits as described in Supplementary Figure S2. As explained in Supplementary Figure S2, K_M^{ATP} values for E^{DNA_1} and E_{DNA_2} (Scheme 1) are not known but needed for the fits. In the fits shown it was postulated that E^{DNA_1} has the same K_M^{ATP} value as free enzyme (1 mM;

Table I) and that the $K_{\mathrm{M}}^{\mathrm{ATP}}$ for $\mathrm{E}_{\mathrm{DNA}_2}$ is the same as that for enzyme with saturating DNA (0.2 mM). Identical estimates of the acceptable values for the parameters analyzed in the Figure were obtained when different combinations of values for $K_{\mathrm{M}\{\mathrm{DNA}_1\}}^{\mathrm{ATP}}$ and $K_{\mathrm{M}\{\mathrm{DNA}_2\}}^{\mathrm{ATP}}$ were used as described in Supplementary Figure S2 ($K_{\mathrm{M}\{\mathrm{DNA}_1\}}^{\mathrm{ATP}} = K_{\mathrm{M}\{\mathrm{DNA}_2\}}^{\mathrm{ATP}} = 1$ mM, $K_{\mathrm{M}\{\mathrm{DNA}_1\}}^{\mathrm{ATP}} = 0.2$ mM and $K_{\mathrm{M}\{\mathrm{DNA}_2\}}^{\mathrm{ATP}} = 1$ mM, or $K_{\mathrm{M}\{\mathrm{DNA}_1\}}^{\mathrm{ATP}} = K_{\mathrm{M}\{\mathrm{DNA}_2\}}^{\mathrm{ATP}} = 0.2$ mM; analysis not shown).

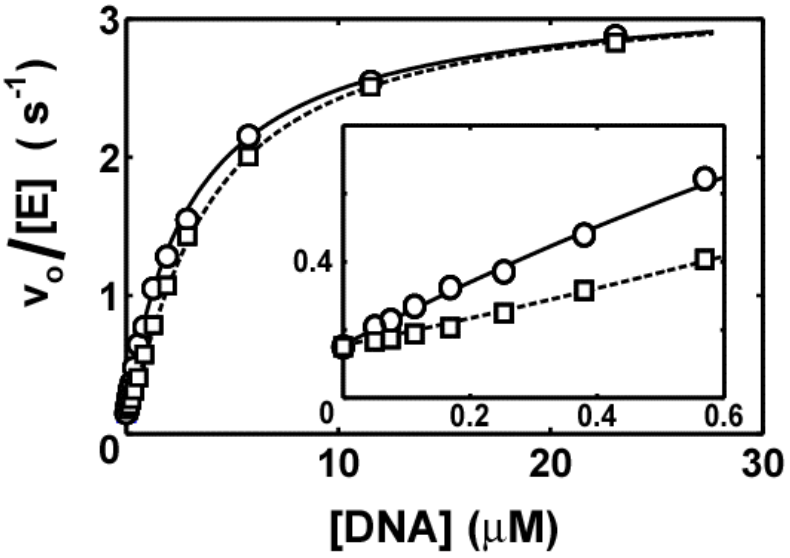

Supplementary Figure S4: ATPase stimulation by a 40 bp DNA duplex with saturating concentrations of Mg^{2+}-ATP (3 mM). A) Dependence of the observed ATP hydrolysis rate constant (v_o / [E]) on the DNA concentration with 13 nM (○) and 650 nM (□) topoisomerase II. Lines represent a global fit of Scheme 1 to the data.

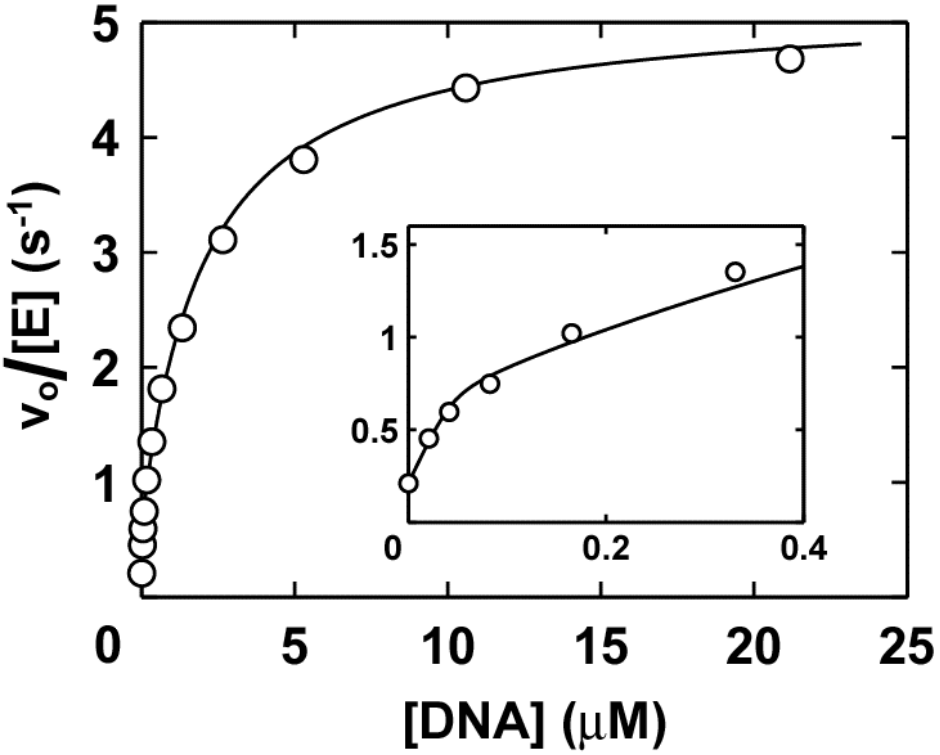

Supplementary Figure S5: Dependence of the observed ATP hydrolysis rate constant (v_o / [E]) of Y782F topoisomerase II (45 nM) on the concentration of the 68 bp DNA duplex with saturating (3 mM) Mg^{2+}-ATP. The line represents a fit of Scheme 1 to the data.

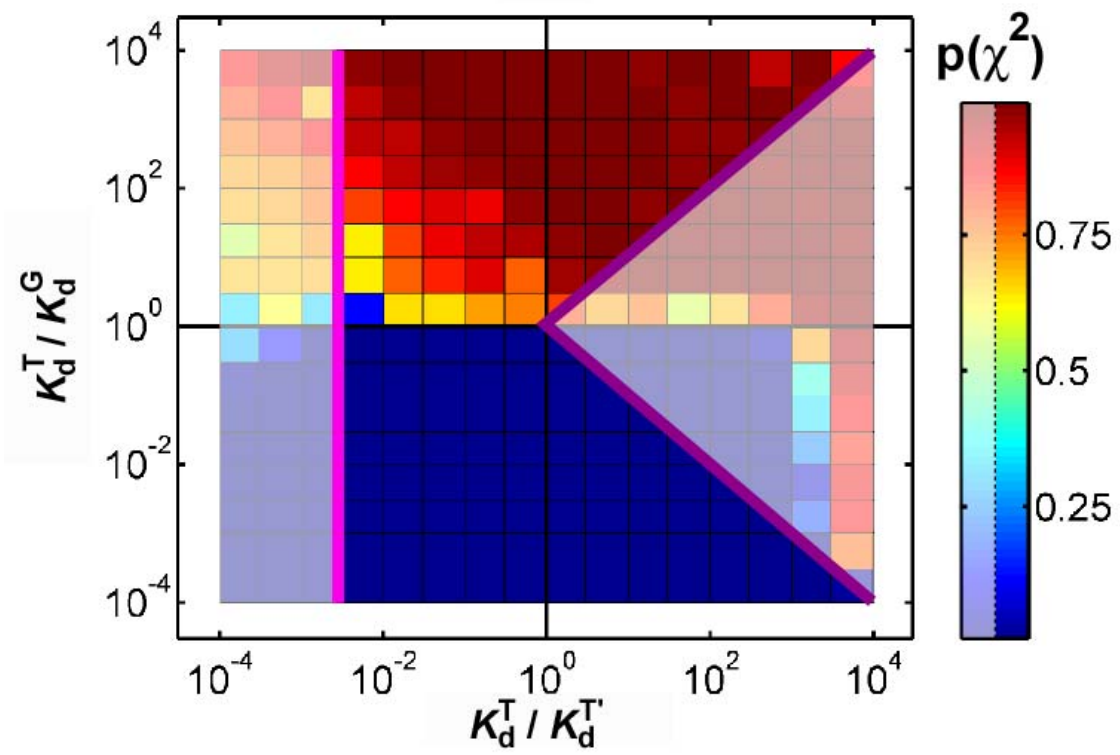

Supplementary Figure S6: Systematic search for models that are consistent with the DNA dependence of the ATPase activity and the topoisomerase II-mediated DNA cleavage with the side condition $K'_{clvg} \geq K_{clvg}$ (Scheme 2). Equilibrium cleavage data obtained at three enzyme concentrations [36 nM (data not shown), 360 nM and 3200 nM (Figure 4)] with varying concentrations of 46 bp duplexes in Mg^{2+}-AMPPNP were globally fit to models that varied in the amount of DNA binding cooperativity ($K_d^T / K_d^{T'}$) and in the relative affinities between the T- and the G-DNA sites (K_d^T / K_d^G). The goodness of the each fit p(χ^2) was estimated by χ^2 statistics. p(χ^2) (see color legend) was plotted on a two dimensional grid spanned by the ratios $K_d^T / K_d^{T'}$ and K_d^T / K_d^G. The area shown in saturated colors in between the magenta and violet lines represents combinations of values that are not ruled out based on the analysis of the DNA dependence of the ATPase reaction. Values located to the left of the magenta line ($K_d^T / K_d^{T'} < 3*10^{-3}$) possess a degree of negative DNA binding cooperativity that is not supported by the ATPase data (Supplementary Figure S3). Values to the right of the violet lines ($K_d^{T'} < K_d^G$ for

$K_d^T > K_d^G$ and $K_d^{G'} < K_d^T$ for $K_d^T < K_d^G$) are ruled out by the ATPase data as this area contains all values with positive, observed DNA binding cooperativity (Supplementary Figure S3 and Table II). The only values that are allowed by the results from the ATPase data (saturated colors) and that can fit the DNA cleavage data [$p(\chi^2) > 0.05$] are values for which the G-DNA site affinity exceeds that of the T-DNA site ($K_d^T / K_d^G > 10^0$).

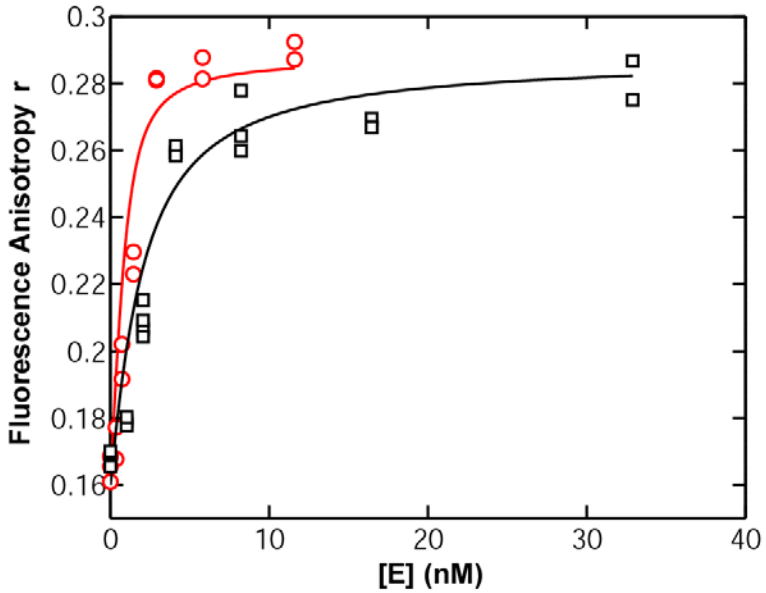

Supplementary Figure S7: Binding of ROX-labeled 40 bp DNA duplex (1 nM) to wild-type (black squares) or Y782F enzyme (red circles) in low salt buffer [25 mM Hepes-KOH pH 7.5, 5 mM $MgCl_2$, 50 mM KCl, 6% glycerol, 5 mM 2-mercaptoethanol]. Lines are fits of the data to the quadratic binding isotherm (Equation 1) to $K_d^{apparent}$ = 1.5 nM (black) and $K_d^{apparent}$ = 0.3 nM (red). However, these $K_d^{apparent}$ values only represent upper limits as the $K_d^{apparent}$ values are close to or lower than the DNA concentration used; i.e. the apparent binding curves represent stoichiometric titrations from which binding constants cannot be obtained.

Interdomain Communication in DNA Topoisomerase II: DNA BINDING AND ENZYME ACTIVATION

Felix Mueller-Planitz and Daniel Herschlag

J. Biol. Chem. 2006, 281:23395-23404.
doi: 10.1074/jbc.M604119200 originally published online June 16, 2006
